Trillian Gregg,[1,2,3] Chetan Poudel,[1,3] Brian A. Schmidt,[1] Rashpal S. Dhillon,[4] Sophia M. Sdao,[5] Nathan A. Truchan,[1] Emma L. Baar,[1] Luis A. Fernandez,[6] John M. Denu,[4] Kevin W. Eliceiri,[3,7] Jeremy D. Rogers,[3,7] Michelle E. Kimple,[1,8] Dudley W. Lamming,[1,8] and Matthew J. Merrins[1,3,4,8]

CrossMark

Pancreatic β-Cells From Mice Offset Age-Associated Mitochondrial Deficiency With Reduced K$_{ATP}$ Channel Activity

ISLET STUDIES

Aging is accompanied by impaired glucose homeostasis and an increased risk of type 2 diabetes, culminating in the failure of insulin secretion from pancreatic β-cells. To investigate the effects of age on β-cell metabolism, we established a novel assay to directly image islet metabolism with NAD(P)H fluorescence lifetime imaging (FLIM). We determined that impaired mitochondrial activity underlies an age-dependent loss of insulin secretion in human islets. NAD(P)H FLIM revealed a comparable decline in mitochondrial function in the pancreatic islets of aged mice (≥24 months), the result of 52% and 57% defects in flux through complex I and II, respectively, of the electron transport chain. However, insulin secretion and glucose tolerance are preserved in aged mouse islets by the heightened metabolic sensitivity of the β-cell triggering pathway, an adaptation clearly encoded in the metabolic and Ca^{2+} oscillations that trigger insulin release (Ca^{2+} plateau fraction: young 0.211 ± 0.006, aged 0.380 ± 0.007, *P* < 0.0001). This enhanced sensitivity is driven by a reduction in K$_{ATP}$ channel conductance (diazoxide: young 5.1 ± 0.2 nS; aged 3.5 ± 0.5 nS, *P* < 0.01), resulting in an ∼2.8 mmol/L left shift in the β-cell glucose threshold. The results demonstrate how mice but not humans are able to successfully compensate for age-associated metabolic dysfunction by adjusting β-cell glucose sensitivity and highlight an essential mechanism for ensuring the maintenance of insulin secretion.

The incidence of type 2 diabetes is disproportionately high in elderly people at >25% compared with 4.1% in younger and 16.2% in middle-aged adults (1). Although insulin resistance and β-cell mass have been extensively studied as contributors to impaired glucose tolerance and diabetes in elderly people (2–4), whether β-cell function contributes to this effect remains uncertain. Confounding our understanding is the misalignment of studies on humans and laboratory mice. A number of reports have indicated that aging mice are resistant to a decline in glucose tolerance and β-cell function (5–8), factors that reportedly decline in humans (2–4,9,10). One potential explanation is that differences in mitochondrial function, which are proposed to underlie the age-related decline of numerous tissues (11), exist between mouse and human β-cells. If β-cells are susceptible to age-related mitochondrial defects, one expects glucose-stimulated insulin secretion (GSIS) to significantly decline, considering that β-cells use metabolism as a signaling pathway not only to trigger oscillations of insulin secretion but also to augment the magnitude of the secretory response through metabolic amplifying

[1]Department of Medicine, Division of Endocrinology, Diabetes, and Metabolism, University of Wisconsin-Madison, Madison, WI
[2]Biophysics Graduate Training Program, University of Wisconsin-Madison, Madison, WI
[3]Laboratory for Optical and Computational Instrumentation, University of Wisconsin-Madison, Madison, WI
[4]Department of Biomolecular Chemistry, University of Wisconsin-Madison, Madison, WI
[5]Integrated Program in Biochemistry, University of Wisconsin-Madison, Madison, WI
[6]Department of Surgery, Division of Transplantation, University of Wisconsin-Madison, Madison, WI
[7]Department of Biomedical Engineering, University of Wisconsin-Madison, Madison, WI
[8]William S. Middleton Memorial Veterans Hospital, Madison, WI

pathways (12). Indeed, age-associated factors intrinsic to the β-cell, including defects in NAD^+ synthesis (13), reduce mitochondrial copy number (14), and epigenomic changes affecting the expression of metabolic genes (7) have been reported, but the extent to which they affect metabolic function in mouse and human β-cells remains unclear.

In this work, we explored the species differences between aging mouse and human β-cells ex vivo to define the effect of age on the intrinsic ability of the β-cell to respond to glucose independently from other age-related physiological changes. We also used this opportunity to develop NAD(P)H fluorescence lifetime imaging (FLIM) as a novel approach to image islet metabolism. This method is more easily interpreted than intensity-based NAD(P)H imaging (15–18), which cannot distinguish increases in NADH production, for example, from the binding of NADH to proteins (which can multiply the fluorescence [19]). Using NAD(P)H FLIM, we report that aged human and mouse β-cells exhibit similar defects in mitochondrial glucose sensing. However, mouse β-cells are uniquely resistant to age-associated defects in insulin secretion, which is maintained in aged mice by the heightened metabolic sensitivity of the β-cell plasma membrane, an effect driven by the reduction of K_{ATP} channel activity.

RESEARCH DESIGN AND METHODS

Human Islets

An exemption was granted for all protocols by the institutional review board at the University of Wisconsin-Madison under protocol number 2015-0356. Human islets were obtained from the Integrated Islet Distribution Program, including the center at the University of Wisconsin. The Integrated Islet Distribution Program isolation protocols and insulin secretion quality control assays can be found at https://iidp.coh.org/investigator_sops .aspx. After shipment, the islets were cultured overnight in RPMI 1640/10% FBS and used within 24 h for insulin secretion measurements.

Mice

All animal studies were approved by the Institutional Animal Care and Use Committees of the University of Wisconsin-Madison and the William S. Middleton Memorial Veterans Hospital. Aged (18-, 24-, and 30-month-old) and young (4- to 6-month-old) C57BL/6J male mice used for the insulin secretion and mitochondrial assays were from the National Institute on Aging (NIA) Aged Rodent Colony. Additional 4- to 6-month-old C57BL/6J male mice used for the calcium and electrophysiology experiments were purchased from The Jackson Laboratory. The median life expectancy of C57BL/6J male mice from these sources is ~28 months (20) (http://phenome.jax.org).

In Vivo Studies

Glucose tolerance tests were performed by fasting the mice overnight for 16 h and then injecting 1 g/kg glucose intraperitoneally; glucose measurements were then performed at the indicated times by using a Bayer Contour blood glucose meter and test strips. In vivo GSIS and fasting insulin levels were determined by fasting the mice overnight for 16 h, measuring blood glucose, and collecting tail blood (using Sarstedt heparinized tubes) immediately before and 15 min after injecting 1 g/kg glucose. Insulin levels in heparinized plasma were determined using Mouse Insulin ELISA kits (Crystal Chem).

Islet Isolation and Adenoviral Infection

The mouse pancreas was inflated through the common bile duct with 3–5 mL of 0.5 mg/mL collagenase (C5138; Sigma) and 0.2 mg/mL BSA (A8806; Sigma) in Hanks' balanced salt solution (HBSS) (Invitrogen), excised, and incubated in a glass vial at 37°C in 5 mL HBSS/BSA/ collagenase solution for 5 min on an orbital shaking water bath (SHKA7000; Thermo Fisher Scientific) at 250 rpm. Beginning 6 min postincubation, the digest was agitated for 20 s at 375 rpm every 2 min until minute 28, washed three times with 30 mL ice-cold HBSS/BSA solution, and pelleted at 50g for 2 min. The pellets were resuspended by vortex at medium speed in 1–2 mL of solution and hand-picked from 60 mL of ice-cold HBSS/BSA solution. After isolation, the islets were maintained in RPMI 1640 supplemented with 10% FBS (volume for volume), 100 units/mL penicillin, and 100 μg/mL streptomycin (Invitrogen). Adenoviruses were used to express PercevalHR ATP/ADP sensors (49082; Addgene) in islet β-cells under control of the rat insulin promoter as in Merrins et al. (21). Groups of 25 freshly isolated islets were immediately infected with 2,000 multiplicity of infection of each adenoviral construct for 2 h in a 95%/5% air/CO_2 incubator at 37°C followed by removal to fresh culture media lacking virus. Islets were imaged after 1–3 days in culture. We confirmed that the presence of the PercevalHR sensors, which were expressed in only a small fraction of β-cells, had no effect on downstream Ca^{2+} oscillations.

Respirometry

After overnight incubation, 150 islets/condition/mouse (six mice/condition) were transferred to a 35-mm Petri dish containing 2 mL of MiR05 (in mmol/L: 0.5 EGTA, 3 $MgCl_2$, 60 lactobionic acid, 20 taurine, 10 KH_2PO_4, 20 HEPES, 110 sucrose, 1% BSA; pH 7.1, adjusted with 5 mol/L KOH) (22) and 5 mg/mL saponin. Preliminary experiments showed that permeabilized islets demonstrated higher coupled respiration rates. Islets were gently rocked in the permeabilization medium for 20 min. After 20 min, the islets were rinsed with fresh MiR05 in the absence of saponin, and then pipetted into an Oxygraph-2k chamber (OROBOROS) containing 2 mL of MiR05 at 37°C. Oxygen electrodes were calibrated to air-saturated MiR05 buffer at 37°C using published oxygen solubilities (23) corrected for local atmospheric pressure. Oxygen concentration and oxygen flux were recorded using DatLab software (OROBOROS). A modified substrate-uncoupler-inhibitor titration protocol based on Votion et al. (24) was applied. Respiratory flux through complex I was measured by

adding 5 mmol/L glutamate and 1 mmol/L malate followed by 1.25 mmol/L ADP to induce oxidative phosphorylation. To assess the integrity of the outer mitochondrial membrane, cytochrome c was added to the chamber (8 μmol/L) (25), and no significant increases in respiration were observed. Damage to the outer mitochondrial membrane during permeabilization would result in a loss of cytochrome c and a large increase in respiration upon the addition of exogenous cytochrome c to the respiration chamber. Convergent electron flow through complexes I and II was measured with the addition of 10 mmol/L succinate, allowing the electron transport system to achieve maximal coupled respiration. Next, a stepwise addition of carbonyl cyanide p-trifluoromethoxyphenylhydrazone was used to completely uncouple mitochondria (0.250 μmol/L initial + 0.250 μmol/L additions). To assess oxygen flux through complex II, 0.5 μmol/L of rotenone was added to inhibit complex I. Finally, electron transfer was blocked at complex III with the addition of 5 μmol/L of antimycin A and allowed to run long enough to obtain a residual oxygen consumption. Oxygen flux was expressed per milligram of total protein (Pierce 660-nm protein assay; Thermo Fisher Scientific).

FLIM of NAD(P)H

Islets were imaged in glass-bottom dishes on a custom-built multiphoton laser scanning system based around a Nikon TE-300 inverted microscope equipped with a Plan Apo 60×/1.4 NA oil immersion objective (Nikon Instruments) in a standard external solution containing (in mmol/L) 135 NaCl, 4.8 KCl, 5 CaCl$_2$, 1.2 MgCl$_2$, 20 HEPES, and 10 glucose (pH 7.35). Temperature was maintained at 35°C by using a LiveCell incubator (Pathology Devices). NAD(P)H was excited with a Mai Tai DeepSee Ti:Sapphire laser (Spectra-Physics) at 740 nm with a 450/70m bandpass emission filter (Chroma) before being collected by a Hamamatsu H7422P-40 GaAsP photomultiplier tube. FLIM images were collected at 256 × 256 resolution with 120 s (1/s) collection using SPC-830 Photon Counting Electronics (Becker & Hickl GmbH). In each experiment, urea crystals were used to define the instrument response function with a 370/10 bandpass emission filter (Chroma), and coumarin was used as a reference for lifetime (2.5 ns) by using a 450/70m bandpass emission filter (Chroma). For analysis, raw SDT files were imported into MATLAB (MathWorks), and a custom script was used to generate a phasor histogram for each treatment by using the equations in Digman et al. (26). To avoid contamination from lipofuscin fluorescence in the aged cells (27), which forms a short lifetime tail in the phasor plot, all data were reported as the phasor histogram peak (1-g_{max},s_{max}).

Time-lapse Imaging of NAD(P)H, ATP/ADP, and Ca^{2+}

For measurements of cytosolic Ca^{2+}, islets were preincubated in 2.5 μmol/L Fura Red (Molecular Probes, Eugene, OR) for 45 min at 37°C. Islets were then placed in an RC-24N glass-bottom chamber (54 μL volume) (Warner Instruments) on a Nikon Eclipse Ti-E inverted microscope equipped with Super Fluor 10×/0.5 NA and 20×/0.75 NA

objectives (Nikon Instruments). The chamber was perfused with standard external solution (as previously described). The flow rate was 0.3 mL/min, and temperature was maintained at 33°C using inline solution and chamber heaters (Warner Instruments). Excitation was provided by a SOLA SE II 365 (lumencor) set to 10% output. Excitation (x) or emission (m) filters (ET type; Chroma Technology) were used in combination with an FF444/521/608-Di01 dichroic beamsplitter (Semrock) as follows: Fura Red 430/20x and 500/20x, 630/70m (R430/500); NAD(P)H 365/20x, 470/24m; and PercevalHR 430/20x and 500/20x, 535/35m (R500/430). Fluorescence emission was collected with a Hamamatsu ORCA-Flash4.0 V2 Digital CMOS camera at 0.125–0.2 Hz. A single region of interest was used to quantify the average response of each islet using Nikon NIS-Elements and MathWorks MATLAB software.

Electrophysiology

β-Cell membrane potential and K$_{ATP}$ conductance were measured as in Ren et al. (28). Briefly, a Sutter MP-225 micromanipulator was used together with a HEKA EPC 10 patch clamp amplifier in the perforated patch clamp configuration to record membrane potential from intact islets perfused with standard external solution (as previously described). Pipette tips were filled with an internal solution (in mmol/L: 28.4 K$_2$SO$_4$, 63.7 KCl, 11.8 NaCl, 1 MgCl$_2$, 20.8 HEPES, 0.5 EGTA, 40 sucrose; pH 7.2) containing 0.36 mg/mL of amphotericin B. Islet β-cells were identified by the presence of slow oscillations in 10 mmol/L glucose. The amplifier was then switched into voltage clamp mode. Conductance changes were determined from the current-voltage relation using 2-s voltage ramps from −120 to −50 mV every 20 s during the silent phase of bursting and following application of 200 μm diazoxide. Assuming that diazoxide acts by maximizing steady-state K$_{ATP}$ open probability, changes in conductance primarily reflect changes in the number of open K$_{ATP}$ channels.

Ex Vivo Insulin Release

The GSIS assay was performed on human and mouse islets by using a high-throughput multiple-well plate technique (29) in which islets were individually incubated in a tissue culture–treated 96-well V-bottom plate, allowed to adhere for 24 h, and incubated with Krebs-Ringer bicarbonate buffer at 1.7 mmol/L glucose (preincubation) followed by a stimulatory 16.7 mmol/L glucose incubation for 45 min each. Secretory medium was then collected, and the islets were lysed with a cell lysis buffer (9803; Cell Signaling Technology). Insulin secretion as a percentage of total islet insulin content was measured by ELISA.

Statistics

Data are expressed as mean ± SE. Statistical significance was determined using one- or two-way ANOVA with Sidak multiple comparisons test post hoc or Student t test as appropriate. Differences were considered to be statistically significant at $P < 0.05$. Statistical calculations were performed with GraphPad Prism software.

RESULTS

Human Aging Is Associated With Defects in GSIS and Islet Metabolism

Insulin secretion measured in islets isolated from 31 human donors ranging in age from 19 to 64 years (Supplementary Table 1) revealed a significant decline in β-cell function with age that was prominent at high glucose levels ($R^2 = 0.51$, $P < 0.0001$) (Fig. 1A). The stimulation index, defined as the fold-change in GSIS, pointed to the same age-related deficiency ($R^2 = 0.26$, $P = 0.0046$) (Fig. 1B). There was no change in insulin content with age (Fig. 1C) or trend in BMI across the donor population (Fig. 1D). Neither the insulin secretion in high glucose nor the stimulation index was correlated with BMI (Fig. 1E and F).
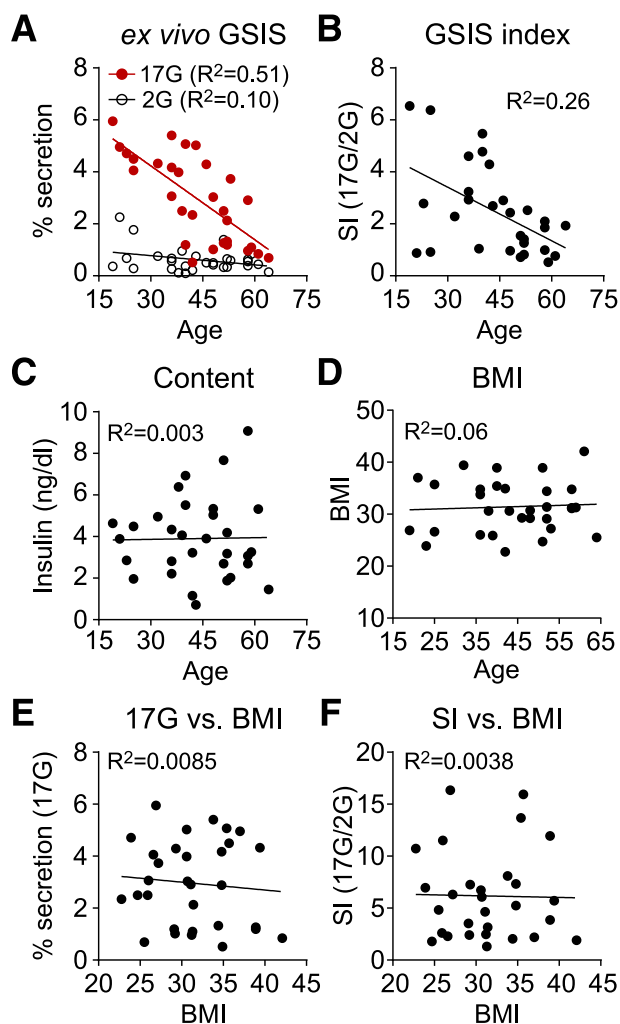
Figure 1—Insulin secretion declines with age in human islets. Insulin secretion (2 mmol/L glucose [2G] and 17 mmol/L glucose [17G]) (A), stimulation index (SI) (i.e., stimulated/basal secretion) (B), insulin content (C), and BMI (D) are shown as a function of donor age (n = 31). E and F: Insulin secretion (17G) and SI as a function of BMI (n = 31). Donor information is listed in Supplementary Table 1.

To ascertain the relationship between insulin secretion and glucose metabolism in these islets, we used multiphoton FLIM of NADH and NADPH to directly image human islet metabolism. Rather than reporting NAD(P)H fluorescence intensity (Fig. 2A, left) (16), FLIM measures the duration that NAD(P)H remains in the excited state (its fluorescence lifetime), which increases approximately sixfold when the coenzymes are bound to protein (19,30). The discrete lifetimes imparted on NADH and NADPH by each of their binding proteins were plotted as phasor histograms (26) so that each distinct mixture of lifetimes occupies a unique position on the plot (Fig. 2A, right). Note that the images of aged islets especially contain lipofuscin puncta (arrows), a cellular waste product identifiable by its broad-spectrum excitation (31) that accumulates with age independently of obesity or diabetes phenotypes (27); on the basis of its very short lifetime, lipofuscin was excluded from the analysis of the phasor histogram peak. Relative to islets from an older donor (58 years old, ACKH054A), the application of 17 mmol/L glucose to islets from a younger donor (24 years old, ACJ3270) shifted the phasor peak significantly further along the abscissa, reflecting an increase in bound NAD(P)H, which has a long lifetime (32). The difference in islet metabolism between aged and young islets was even more pronounced at 2 mmol/L glucose (Fig. 2B and C). A shift in the histogram peaks toward free NADH was induced by rotenone, which blocks NADH utilization at complex I and serves as a positive control to calibrate the FLIM. Changes in the islet phasor histogram peak along the $1\text{-}g_{max}$ axis reflect the metabolic consequences of activating/inactivating the electron transport chain, consistent with NAD(P)H FLIM studies that used alternative electron transport chain inhibitors (e.g., KCN [32,33]). Of note, donor age was correlated with the progressive loss of glucose-dependent NADH utilization ($R^2 = 0.63$, $P = 0.006$) (Fig. 2D), indicating that a reduction in mitochondrial metabolism contributes to the loss of insulin secretion with age.

Despite Mitochondrial Decline, Insulin Secretion and Glucose Tolerance Are Preserved in Aged Mice

Given the strong relationship between β-cell secretory dysfunction and human aging, we investigated organismal glucose homeostasis in young (4- to 6-month-old), middle-aged (18-month-old), and aged (≥24-month-old) C57BL/6J mice from the NIA Aged Rodent Colony. Glucose tolerance, measured in fasted animals, was equivalent between the young and aged mice (Fig. 3A and B) as reported previously (5,8). However, middle-aged and aged animals trended toward increased fasting insulin levels, and aged animals exhibited an augmented insulin secretory response after intraperitoneal glucose injection (Fig. 3C and D). To determine whether this effect can be explained by a β-cell autonomous mechanism, pancreatic islets isolated from young and aged mice were subjected to an ex vivo GSIS assay. Islets from the aged mice secreted significantly more insulin than islets from young
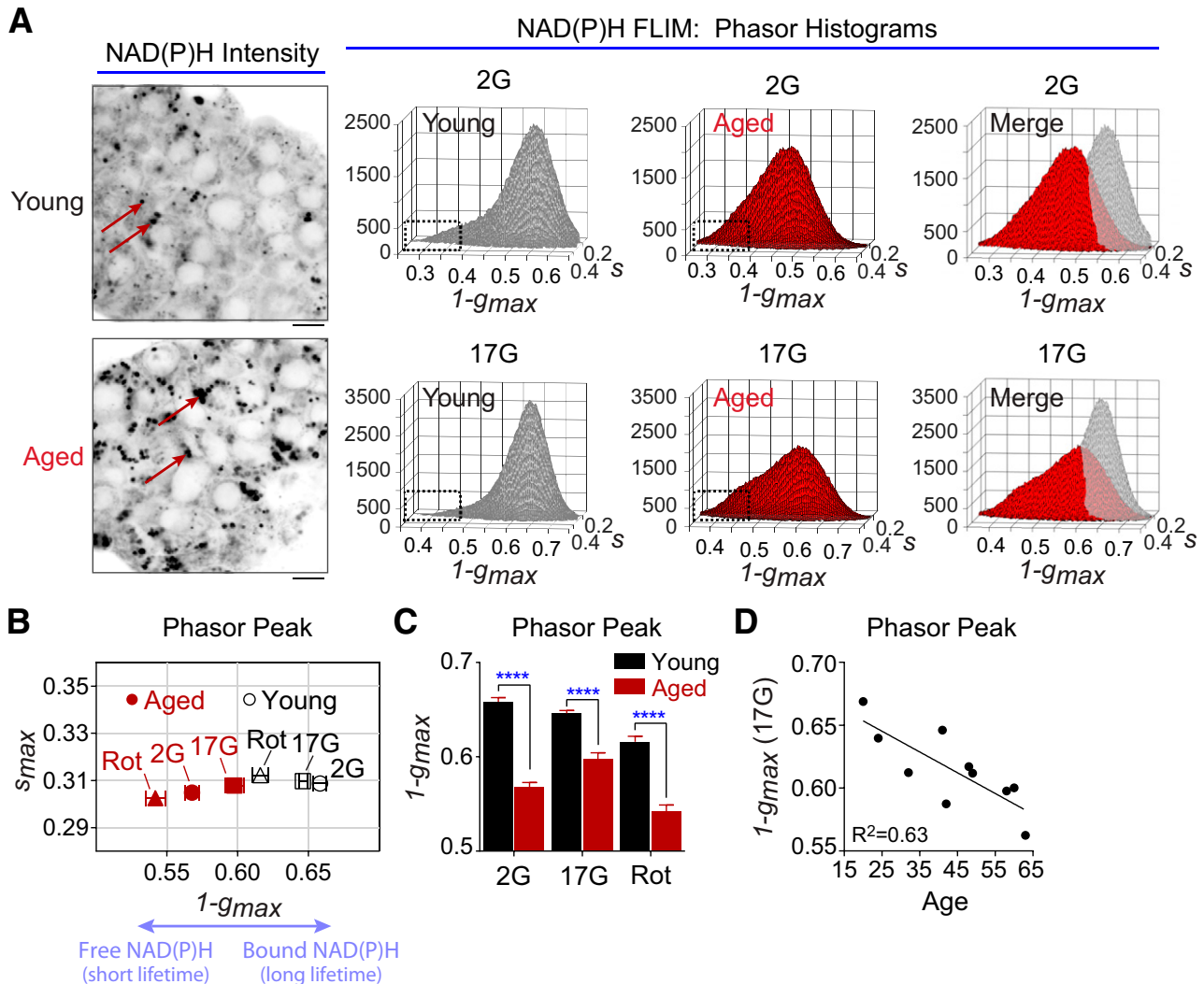
Figure 2—NAD(P)H FLIM of human islet metabolism. *A*: Multiphoton FLIM of NAD(P)H in human islets from representative young (24-year-old, ACJ3270) and aged (58-year-old, ACKH054A) donors. Phasor histograms show the frequency distribution of NAD(P)H lifetimes in young and aged islets (20 islets each). Lipofuscin (arrows) was excluded from the FLIM analysis on the basis of its very short lifetime, which forms a tail at the left of the phasor plots (boxes). Scale bar = 5 μm. *B* and *C*: Translation of the phasor histogram peaks ($1\text{-}g_{max}, s_{max}$) along the $1\text{-}g_{max}$ axis were used to quantify changes in bound:free NAD(P)H in response to 2 mmol/L glucose (2G), 17 mmol/L glucose (17G), and 17G plus 5 μmol/L rotenone (Rot) (complex I inhibitor). $1\text{-}g_{max}$ is plotted to give the same directionality as mitochondrial oxygen consumption. Data are mean $\pm$ SEM and were compared by two-way ANOVA with Sidak posttest. ****$P < 0.0001$. *D*: Islet mitochondrial response to 17G declines with age. Data are 20 islets from each of 10 human islet donors (ACJV399A, ACJY368C, ACJ3270, ACKB319, ACKB044, ACKB010B, ACKH054A, ADAH342, ADAN146A, ADAT167). Donor information is listed in Supplementary Table 1.

mice at both basal and stimulatory glucose concentrations (Fig. 3*E*); no difference in insulin content was observed (data not shown). These data, which align with recent reports (7,34), imply that β-cell compensation is necessary to maintain euglycemia in aged mice, which could reflect increased β-cell mass (islet area was 43% larger in the aged mice relative to controls [Fig. 3*F*]) as well as functional compensation.

As a means to compare metabolic function in young and aged mice with the human islet phenotype, multiphoton NAD(P)H FLIM was again used to directly image mitochondrial metabolism (Fig. 4). Although glucose induced an

increase in free NAD(P)H in both groups, quantification of the phasor histogram peaks showed that the NAD(P)H response is depressed in the aged islets in response to glucose (Fig. 4*A* and *B*). NADH consumption by the mitochondrial respiratory chain was assessed by acute application of rotenone (5 μmol/L, complex I inhibitor) and oligomycin (5 μmol/L, complex V inhibitor). In all four treatments, a decline in mitochondrial function (reflected by the decline in bound NAD[P]H) was evident in aged islets relative to young control islets (Fig. 4*C*). The relative difference in the cellular response to oligomycin and rotenone, which reveals the proton leak (35), was not altered.
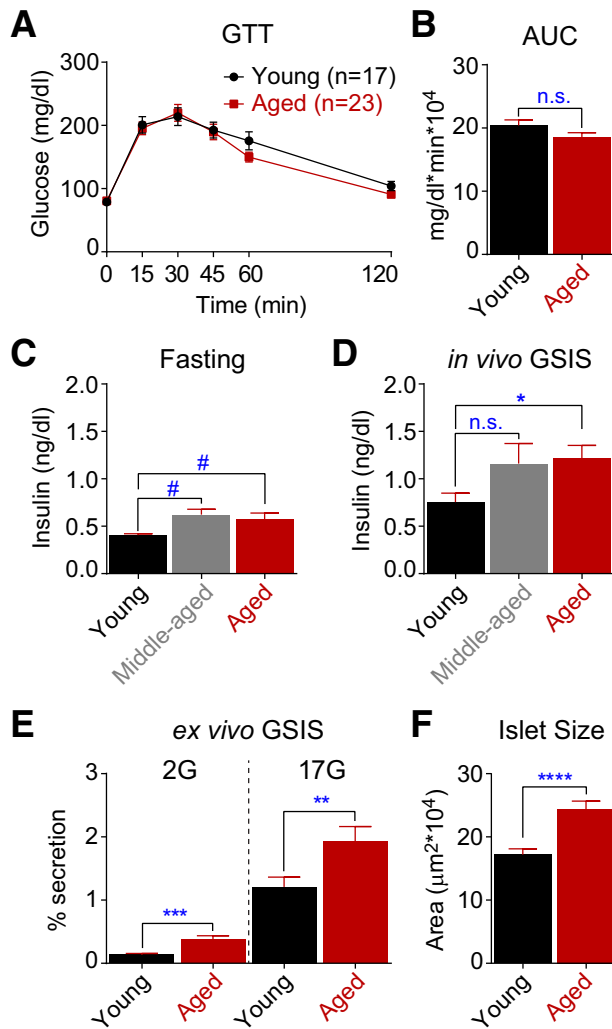
Figure 3—Insulin secretion is increased in aged mice. In vivo glucose tolerance (*A* and *B*) in young (6-month-old) and aged (≥24-month-old) C57BL/6J mice. *C* and *D*: Plasma insulin levels in young (6-month-old, *n* = 5), middle-aged (18-month-old, *n* = 5), and aged (≥24-month-old, *n* = 10) mice after an overnight fast before (*C*) and 15 min after (*D*) intraperitoneal glucose injection. *E*: Insulin secretion measured ex vivo using islets from young (*n* = 2) and aged (*n* = 2) mice. *F*: Islet size was estimated from the cross-sectional area. Young, 103 islets from 2 mice; aged, 122 islets from five mice. Data are mean ± SEM and were compared by *t* test (*A–D* and *F*) or ANOVA with Sidak posttest (*E*). #*P* = 0.07; **P* < 0.05; ***P* < 0.01; ****P* < 0.001; *****P* < 0.0001. AUC, area under the curve; GTT, glucose tolerance test; n.s., not significant.

As a second approach, we measured mitochondrial oxygen consumption in permeabilized islets stimulated with glutamate, malate, succinate, and ADP. In excellent agreement with the NAD(P)H FLIM, mitochondrial respiration was strongly decreased in the aged islets (Fig. 4*D*). Flux through complexes I and II was similarly reduced (by 52% and 57%, respectively), indicating that defects in aged cells manifest within the electron transport chain. Because age-associated mitochondrial dysfunction afflicts both human and mouse islets, these findings

prompted us to seek an explanation for the augmented insulin secretion we observed in aged mice.

Hypersensitivity of the β-Cell Plasma Membrane, Driven by a Reduction in K_{ATP} Conductance, Compensates for Mitochondrial Dysfunction in Aged Mice

Downstream of the mitochondria, ATP/ADP, K_{ATP} channels, and Ca^{2+} control the triggering pathway of insulin secretion. Oscillations in these parameters between active and silent phases occur within an intermediate range of glucose levels (Fig. 5*A*). Within this range, an analysis of the oscillatory plateau fraction (the fraction of the time the islet spends in the active state [21,36,37]) can provide direct information on the β-cell glucose threshold without the need for a full glucose dose-response curve. This is because of the direct relationship between β-cell glucose metabolism and plateau fraction, which can be calculated from ATP/ADP or Ca^{2+} oscillations (Fig. 5*B*). Note that increased ATP/ADP plateau fraction does not equal increased ATP level; the plateau fraction of ATP/ADP follows the activity of membrane potential oscillations strictly (21), whereas the plateau fraction of Ca^{2+} oscillations (in the same islet) is slightly longer due to extended Ca^{2+} release from the endoplasmic reticulum (ER) during the silent phase (38).

When measured simultaneously, Ca^{2+} and ATP/ADP oscillations in mouse islets (Fig. 5*C*) are out of phase because of ATP consumption by Ca^{2+}-ATPases located in the ER and plasma membrane (39,40). Compared with young islets, aged islets displayed an increased oscillatory plateau fraction, reflecting increased sensitivity to glucose (Fig. 5*D*); based on data shown in Fig. 5*B*, we estimated that this effect corresponds to an ~2.8 mmol/L left shift in the plasma membrane glucose threshold. Although enhanced insulin secretion is consistent with enhanced Ca^{2+} activity in aged β-cells (Fig. 3), this observation was unexpected because of the respiratory chain failure we observed in the aged mouse islets (Fig. 4), which would be expected to restrict K_{ATP} channel inhibition and Ca^{2+} channel activation. These findings suggest that the β-cell plasma membrane in aged cells is hypersensitive to glucose metabolism.

Because K_{ATP} channels are the primary metabolic sensor for the β-cell plasma membrane (41,42), we hypothesized that the loss of K_{ATP} channel conductance (G_{KATP}) could account for the enhanced Ca^{2+} oscillations we observed in aged islets. G_{KATP} was calculated from voltage ramps (28) during islet bursting and in the presence of the K_{ATP} channel opener diazoxide (200 μmol/L) (Fig. 5*E*). The more K_{ATP} channels present in the plasma membrane, the larger the change in G_{KATP} seen in response to diazoxide; by this measure, G_{KATP} was reduced by 31% in aged relative to young β-cells (Fig. 5*F*, left). There was no difference in cell size between groups (data not shown). We also confirmed that these results were not due to differences in leak resistance between individual islets by subtracting the conductances measured during the
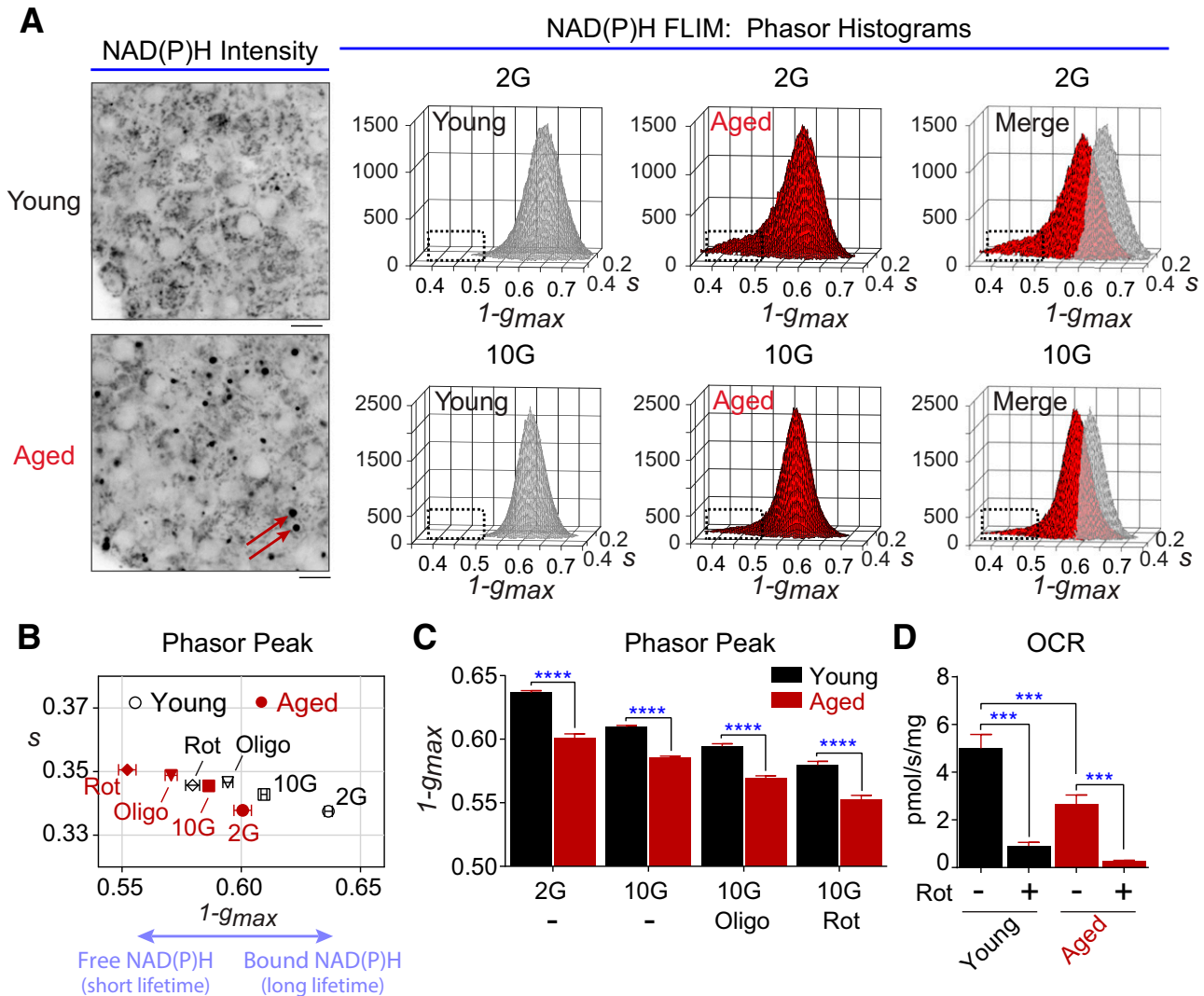
Figure 4—NAD(P)H FLIM of mouse islet metabolism. *A*: Multiphoton FLIM of NAD(P)H in islets isolated from young (6-month-old) and aged (30-month-old) C57BL/6J mice. Arrows in the NAD(P)H intensity images indicate contaminating lipofuscin fluorescence. Scale bar = 5 μm. Phasor histograms show the frequency distribution of NAD(P)H lifetimes in young and aged islets in the presence of 2 mmol/L glucose (2G) and 10 mmol/L glucose (10G) (10 islets per condition). *B* and *C*: Translation of the phasor histogram peaks ($1-g_{max}, s_{max}$) along the abscissa were used to quantify changes in bound:free NAD(P)H in response to 2G, 10G, and 10G plus 5 μmol/L oligomycin (Oligo) (complex V inhibitor) or 5 μmol/L rotenone (Rot) (complex I inhibitor), as indicated. *D*: Oxygen consumption rate (OCR) measured from five mice per condition (150 islets per mouse) shows that stimulated mitochondrial respiration is deficient in aged islets. Rot (5 μmol/L) was present as indicated. Data are mean ± SEM and were compared by ANOVA with Sidak posttest. ***$P < 0.001$; ****$P < 0.0001$.

silent phase of bursting from the same β-cell during diazoxide application, which yielded the same fundamental conclusion (Fig. 5*F*, right). The age-dependent loss of K_{ATP} channels would be expected to reduce the ATP/ADP ratio required to initiate membrane depolarization and account for the enhanced plateau fraction of calcium oscillations and elevated insulin release we observed in aged islets.

DISCUSSION

The focus of this work was to compare the effects of age on β-cell metabolism and insulin secretion in mouse and human islets. To do so, we developed a novel assay for metabolic fingerprinting of the pancreatic islet, NAD(P)H

FLIM. We demonstrated that both human and mouse islets exhibited an age-associated decline in mitochondrial NADH utilization due to defects in the electron transport chain. Of note, we found that islets from aged mice significantly compensated for this defect with restricted β-cell G_{KATP}, which in turn increased the glucose sensitivity of plasma membrane Ca^{2+} triggering and insulin secretion. Although the results help to explain the resistance of mice to age-induced defects in insulin secretion, human islets apparently lack this compensation.

Human aging is accompanied by declining glucose tolerance (2–4), and we detected a corresponding defect
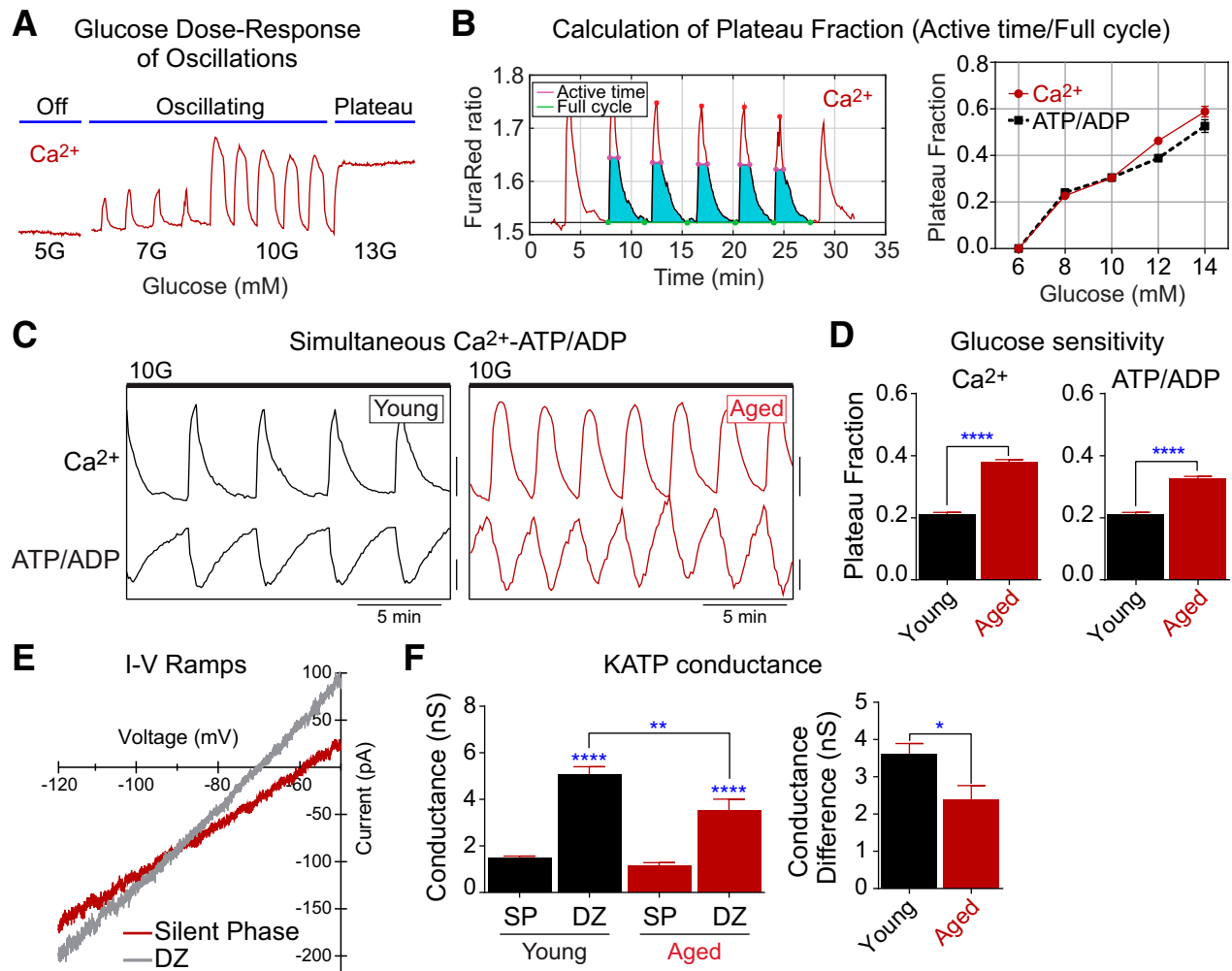
Figure 5—Loss of K_{ATP} channel conductance underlies a left shift in the glucose threshold of aged mouse β-cells. *A*: Recording of islet Ca^{2+} in response to increased glucose levels. *B*: Glucose dependence of plateau fraction calculated from simultaneous recordings of Ca^{2+} (Fura Red) and ATP/ADP (PercevalHR) oscillations using MATLAB. *C*: Ca^{2+} and ATP/ADP oscillations in young (6-month-old) and aged (24-month-old) C57BL/6J mouse islet β-cells in the presence of 10 mmol/L glucose (10G). *D*: The oscillatory plateau fraction, reflecting the plasma membrane glucose sensitivity, was calculated as the fraction of time spent in the active state of each oscillation. Young, 124 islets from four mice; aged, 210 islets from five mice. *E* and *F*: Representative current-voltage relation (I-V) curves showing slope conductance changes in islet β-cells during the silent phase (SP) of bursting (10G) and 5 min after treatment with 200 μmol/L diazoxide (DZ). Average K_{ATP} conductance as well as conductance difference (DZ – SP) were reduced in aged β-cells (eight cells from three mice) relative to young controls (19 cells from four mice). Data are mean ± SEM and were compared by two-way ANOVA with Sidak posttest. *$P < 0.05$; **$P < 0.01$; ****$P < 0.0001$.

in insulin secretion in pancreatic islets isolated from aged human subjects. Of note, our measurements revealed an age-dependent defect in stimulated insulin secretion (R^2 = 0.51, $P < 0.0001$), with a much weaker effect on the stimulation index (R^2 = 0.26, $P = 0.0046$). A decline in the stimulation index based instead on an age-dependent increase in basal insulin secretion has also been reported (9,10), whereas another study found no age-related defects (5). Although we find no fault with these studies, or a satisfactory explanation for the discrepancy between them, our results are qualitatively similar to those of an unpublished study by Benninger and colleagues (R. Benninger, personal communication) that showed a significant age-dependent decline in both stimulated

and basal insulin secretion (21 preparations); in our study, basal secretion trended lower with age but was not significant ($P = 0.08$, 31 preparations).

Studies of glucose homeostasis in aged mice are more consistent. The widely studied C57BL/6 inbred mouse strain exhibits normal glucose tolerance with age (Fig. 3) (5,6,43,44), and in addition to the current study, three reports of mice from the NIA Aged Rodent Colony found that insulin secretion increases with age (Fig. 3) (5,7,8). What, then, explains the discrepant phenotype of human and mouse islets? We considered the possibility that mitochondrial health, which declines with age in human β-cells (14), might be unaffected in mouse islets. However, using NAD(P)H FLIM, we showed that mitochondrial

NADH utilization declines with age in both species (Figs. 2 and 4). Using respirometry, we directly identified defects in complexes I and II of the electron transport chain, which likely underlie the impairment in glucose-dependent hyperpolarization of the mitochondrial membrane potential in aged C57BL/6J mouse islets (6). However, by quantifying the dynamics of glucose-dependent β-cell oscillations in metabolism and Ca^{2+}, we discovered that these age-associated defects in metabolism are compensated for by hypersensitivity of the mouse β-cell plasma membrane. The mechanism of this effect was specifically due to a reduction in K_{ATP} channel conductance, which was accompanied by increased insulin secretion.

The appeal of an age-dependent shift in the β-cell glucose threshold is that insulin secretion can increase despite defects in mitochondrial respiration. Two lines of evidence might explain how regulation of K_{ATP} occurs. The first is based on experiments demonstrating that exposure of islets to hyperglycemic conditions can reduce β-cell K_{ATP} conductance by adjusting K_{ATP} channel trafficking to the plasma membrane (45,46). This trafficking mechanism requires autocrine feedback of insulin (46), which is reminiscent of a second potential mechanism involving insulin-dependent transcriptional regulation of K_{ATP}. In this case, insulin receptor signaling activates cyclin-dependent kinase 4 (Cdk4), which phosphorylates Rb to activate the E2F transcription factors required for Kir6.2 (KCNJ11) promoter activity (47). By activating Kir6.2, which comprises the pore-forming subunits of K_{ATP}, the insulin receptor signaling pathway limits β-cell excitability. Several groups have demonstrated that β-cells exhibit increased expression of cell cycle inhibitors with age (reviewed in Gunasekaran and Gannon [3]), most prominently the Cdk4 inhibitor p16/Ink4a (34,48), which would be expected to restrict E2F activation and Kir6.2 transcription. In this second model, the reduced K_{ATP} channel activity we observed in mouse islets is an inevitable but welcome adaptation to β-cell senescence. Ultimately, however, distinguishing between these two alternative models will require additional experimentation in genetically modified aged mice (e.g., mice lacking Cdk4).

In addition to advancing our understanding of β-cell aging, we have made a significant technical leap by using FLIM of NAD(P)H to quantify the metabolic health of islet cells. Although we do not currently possess a way to distinguish between the endocrine cell types, NAD(P)H FLIM addressed a number of issues inherent to the intensity-based NAD(P)H measurements used in our prior studies (49,50). First, the autofluorescence signal in aged islets is dominated by lipofuscin, which accumulates with age (27). We were able to exclude lipofuscin from our analysis by its short lifetime through the phasor approach to FLIM (26,32); because lipofuscin is accumulated by many cell types in aging rodents and humans, we expect this approach to be broadly applicable to the study of metabolism in other tissues. Second, we noted that NAD(P)H fluorescence intensity, when determined using epifluorescence, strongly depends on islet size. Size matching would have skewed our comparison of young and aged islets, which were 42% larger, and would be impossible when studying islets isolated from some genetic models of obesity, such as *ob/ob* mice. Islet size is normalized when using multiphoton microscopy, which ensures that a uniform volume is measured from each islet.

As the population ages, it seems likely that the already high prevalence of diabetes among older people will continue to rise. In this work, we determined that a reduction in the β-cell glucose threshold allows mice, but apparently not humans of the studied age-group, to circumvent age-associated mitochondrial decline and maintain insulin secretion. This left shift in the glucose threshold for Ca^{2+} activation may also be found in studies of genetic (*db/db*), pharmacologic (streptozotocin), and diet-induced diabetes models (51,52), hinting that threshold shifting is an important mechanism of β-cell compensation for all ages.

References

1. Center for Disease Control and Prevention. 2014 National Diabetes Statistics Report [Internet], 2014. Available from: http://www.cdc.gov/diabetes/data/statistics/2014StatisticsReport.html. Accessed 9 March 2015

2. Chang AM, Halter JB. Aging and insulin secretion. Am J Physiol Endocrinol Metab 2003;284:E7–E12

3. Gunasekaran U, Gannon M. Type 2 diabetes and the aging pancreatic beta cell. Aging (Albany, NY) 2011;3:565–575

4. Kushner JA. The role of aging upon β cell turnover. J Clin Invest 2013;123:990–995

5. Almaça J, Molina J, Arrojo E Drigo R, et al. Young capillary vessels rejuvenate aged pancreatic islets. Proc Natl Acad Sci U S A 2014;111:17612–17617

6. Li L, Trifunovic A, Köhler M, et al. Defects in β-cell Ca^{2+} dynamics in age-induced diabetes. Diabetes 2014;63:4100–4114

7. Avrahami D, Li C, Zhang J, et al. Aging-dependent demethylation of regulatory elements correlates with chromatin state and improved β cell function. Cell Metab 2015;22:619–632

8. Naidoo N, Davis JG, Zhu J, et al. Aging and sleep deprivation induce the unfolded protein response in the pancreas: implications for metabolism. Aging Cell 2014;13:131–141

9. Iozzo P, Beck-Nielsen H, Laakso M, Smith U, Yki-Järvinen H, Ferrannini E; European Group for the Study of Insulin Resistance. Independent influence of age on basal insulin secretion in nondiabetic humans. J Clin Endocrinol Metab 1999;84:863–868

10. Ihm S-H, Matsumoto I, Sawada T, et al. Effect of donor age on function of isolated human islets. Diabetes 2006;55:1361–1368

11. Khrapko K, Vijg J. Mitochondrial DNA mutations and aging: devils in the details? Trends Genet 2009;25:91–98

12. Henquin J-C. The dual control of insulin secretion by glucose involves triggering and amplifying pathways in β-cells. Diabetes Res Clin Pract 2011;93(Suppl. 1):S27–S31

13. Yoshino J, Mills KF, Yoon MJ, Imai S. Nicotinamide mononucleotide, a key NAD(+) intermediate, treats the pathophysiology of diet- and age-induced diabetes in mice. Cell Metab 2011;14:528–536

14. Cree LM, Patel SK, Pyle A, et al. Age-related decline in mitochondrial DNA copy number in isolated human pancreatic islets. Diabetologia 2008;51:1440–1443

15. Patterson GH, Knobel SM, Arkhammar P, Thastrup O, Piston DW. Separation of the glucose-stimulated cytoplasmic and mitochondrial NAD(P)H responses in pancreatic islet beta cells. Proc Natl Acad Sci U S A 2000;97:5203–5207

16. Rocheleau JV, Head WS, Piston DW. Quantitative NAD(P)H/flavoprotein autofluorescence imaging reveals metabolic mechanisms of pancreatic islet pyruvate response. J Biol Chem 2004;279:31780–31787

17. Luciani DS, Misler S, Polonsky KS. Ca2+ controls slow NAD(P)H oscillations in glucose-stimulated mouse pancreatic islets. J Physiol 2006;572:379–392

18. Quesada I, Todorova MG, Soria B. Different metabolic responses in alpha-, beta-, and delta-cells of the islet of Langerhans monitored by redox confocal microscopy. Biophys J 2006;90:2641–2650

19. Lakowicz JR, Szmacinski H, Nowaczyk K, Johnson ML. Fluorescence lifetime imaging of free and protein-bound NADH. Proc Natl Acad Sci U S A 1992;89:1271–1275

20. Turturro A, Witt WW, Lewis S, Hass BS, Lipman RD, Hart RW. Growth curves and survival characteristics of the animals used in the Biomarkers of Aging Program. J Gerontol A Biol Sci Med Sci 1999;54:B492–B501

21. Merrins MJ, Poudel C, McKenna JP, et al. Phase analysis of metabolic oscillations and membrane potential in pancreatic islet β-cells. Biophys J 2016;110:691–699

22. Gnaiger E, Kuznetsov AV. Mitochondrial respiration at low levels of oxygen and cytochrome c. Biochem Soc Trans 2002;30:252–258

23. Forstner H, Gnaiger E. Calculation of equilibrium oxygen concentration. In *Polarographic Oxygen Sensors: Aquatic and Physiological Applications*. Gnaiger E, Forstner H, Eds. New York, Springer, 1983, p. 321–333

24. Votion D-M, Gnaiger E, Lemieux H, Mouithys-Mickalad A, Serteyn D. Physical fitness and mitochondrial respiratory capacity in horse skeletal muscle. PLoS One 2012;7:e34890

25. Kuznetsov AV, Schneeberger S, Seiler R, et al. Mitochondrial defects and heterogeneous cytochrome c release after cardiac cold ischemia and reperfusion. Am J Physiol Heart Circ Physiol 2004;286:H1633–H1641

26. Digman MA, Caiolfa VR, Zamai M, Gratton E. The phasor approach to fluorescence lifetime imaging analysis. Biophys J 2008;94:L14–L16

27. Cnop M, Hughes SJ, Igoillo-Esteve M, et al. The long lifespan and low turnover of human islet beta cells estimated by mathematical modelling of lipofuscin accumulation. Diabetologia 2010;53:321–330

28. Ren J, Sherman A, Bertram R, et al. Slow oscillations of KATP conductance in mouse pancreatic islets provide support for electrical bursting driven by metabolic oscillations. Am J Physiol Endocrinol Metab 2013;305:E805–E817

29. Truchan NA, Brar HK, Gallagher SJ, Neuman JC, Kimple ME. A single-islet microplate assay to measure mouse and human islet insulin secretion. Islets. 2015;7:e1076607

30. Blinova K, Levine RL, Boja ES, et al. Mitochondrial NADH fluorescence is enhanced by complex I binding. Biochemistry 2008;47:9636–9645

31. Marmorstein AD, Marmorstein LY, Sakaguchi H, Hollyfield JG. Spectral profiling of autofluorescence associated with lipofuscin, Bruch's Membrane, and sub-RPE deposits in normal and AMD eyes. Invest Ophthalmol Vis Sci 2002;43:2435–2441

32. Wright BK, Andrews LM, Markham J, et al. NADH distribution in live progenitor stem cells by phasor-fluorescence lifetime image microscopy. Biophys J 2012;103:L7–L9

33. Pate KT, Stringari C, Sprowl-Tanio S, et al. Wnt signaling directs a metabolic program of glycolysis and angiogenesis in colon cancer. EMBO J 2014;33:1454–1473

34. Helman A, Klochendler A, Azazmeh N, et al. p16(Ink4a)-induced senescence of pancreatic beta cells enhances insulin secretion. Nat Med 2016;22:412–420

35. Wikstrom JD, Sereda SB, Stiles L, et al. A novel high-throughput assay for islet respiration reveals uncoupling of rodent and human islets. PLoS One 2012;7:e33023

36. Nunemaker CS, Bertram R, Sherman A, Tsaneva-Atanasova K, Daniel CR, Satin LS. Glucose modulates [Ca2+]i oscillations in pancreatic islets via ionic and glycolytic mechanisms. Biophys J 2006;91:2082–2096

37. Henquin JC. Regulation of insulin secretion: a matter of phase control and amplitude modulation. Diabetologia 2009;52:739–751

38. Ravier MA, Daro D, Roma LP, et al. Mechanisms of control of the free Ca2+ concentration in the endoplasmic reticulum of mouse pancreatic β-cells: interplay with cell metabolism and [Ca2+]c and role of SERCA2b and SERCA3. Diabetes 2011;60:2533–2545

39. Detimary P, Gilon P, Henquin JC. Interplay between cytoplasmic Ca2+ and the ATP/ADP ratio: a feedback control mechanism in mouse pancreatic islets. Biochem J 1998;333:269–274

40. Li J, Shuai HY, Gylfe E, Tengholm A. Oscillations of sub-membrane ATP in glucose-stimulated beta cells depend on negative feedback from Ca(2+). Diabetologia 2013;56:1577–1586

41. Henquin JC. ATP-sensitive K+ channels may control glucose-induced electrical activity in pancreatic B-cells. Biochem Biophys Res Commun 1988;156:769–775

42. Nichols CG. KATP channels as molecular sensors of cellular metabolism. Nature 2006;440:470–476

43. Leiter EH, Premdas F, Harrison DE, Lipson LG. Aging and glucose homeostasis in C57BL/6J male mice. FASEB J 1988;2:2807–2811

44. Lamming DW, Mihaylova MM, Katajisto P, et al. Depletion of Rictor, an essential protein component of mTORC2, decreases male lifespan. Aging Cell 2014;13:911–917

45. Ma Z, Portwood N, Brodin D, Grill V, Björklund A. Effects of diazoxide on gene expression in rat pancreatic islets are largely linked to elevated glucose and potentially serve to enhance beta-cell sensitivity. Diabetes 2007;56:1095–1106

46. Glynn E, Thompson B, Vadrevu S, et al. Chronic glucose exposure systematically shifts the oscillatory threshold of mouse islets: experimental evidence

for an early intrinsic mechanism of compensation for hyperglycemia. Endocrinology 2016;157:611–623

47. Annicotte J-S, Blanchet E, Chavey C, et al. The CDK4-pRB-E2F1 pathway controls insulin secretion. Nat Cell Biol 2009;11:1017–1023

48. Krishnamurthy J, Ramsey MR, Ligon KL, et al. p16INK4a induces an age-dependent decline in islet regenerative potential. Nature 2006;443: 453–457

49. Merrins MJ, Fendler B, Zhang M, Sherman A, Bertram R, Satin LS. Metabolic oscillations in pancreatic islets depend on the intracellular Ca2+ level but not Ca2+ oscillations. Biophys J 2010;99:76–84

50. Merrins MJ, Van Dyke AR, Mapp AK, Rizzo MA, Satin LS. Direct measurements of oscillatory glycolysis in pancreatic islet β-cells using novel fluorescence resonance energy transfer (FRET) biosensors for pyruvate kinase M2 activity. J Biol Chem 2013;288:33312–33322

51. Soria B, Martín F, Andreu E, Sanchez-Andrés JV, Nacher V, Montana E. Diminished fraction of blockable ATP-sensitive K+ channels in islets transplanted into diabetic mice. Diabetes 1996;45:1755–1760

52. Erion KA, Berdan CA, Burritt NE, Corkey BE, Deeney JT. Chronic exposure to excess nutrients left-shifts the concentration dependence of glucose-stimulated insulin secretion in pancreatic β-cells. J Biol Chem 2015;290:16191–16201